Supporting Information for: Plasmonic Vortex Cavities Toward the Ultra-Compact Limit

Da-Jie Yang,† Jing-Yi Wang,† Yuanjie Yang,*,‡ and Yonghui Tian*,†,¶

†*School of Mathematics and Physics, North China Electric Power University, Beijing 102206, China*

‡*School of Physics, University of Electronic Science and Technology of China, Chengdu 611731, China*

¶*School of Physical Science and Technology, Lanzhou University, Lanzhou, Gansu, 730000 China*

E-mail: dr.yang2003@uestc.edu.cn; tianyh@lzu.edu.cn

1. Plasmonic Vortex Lens

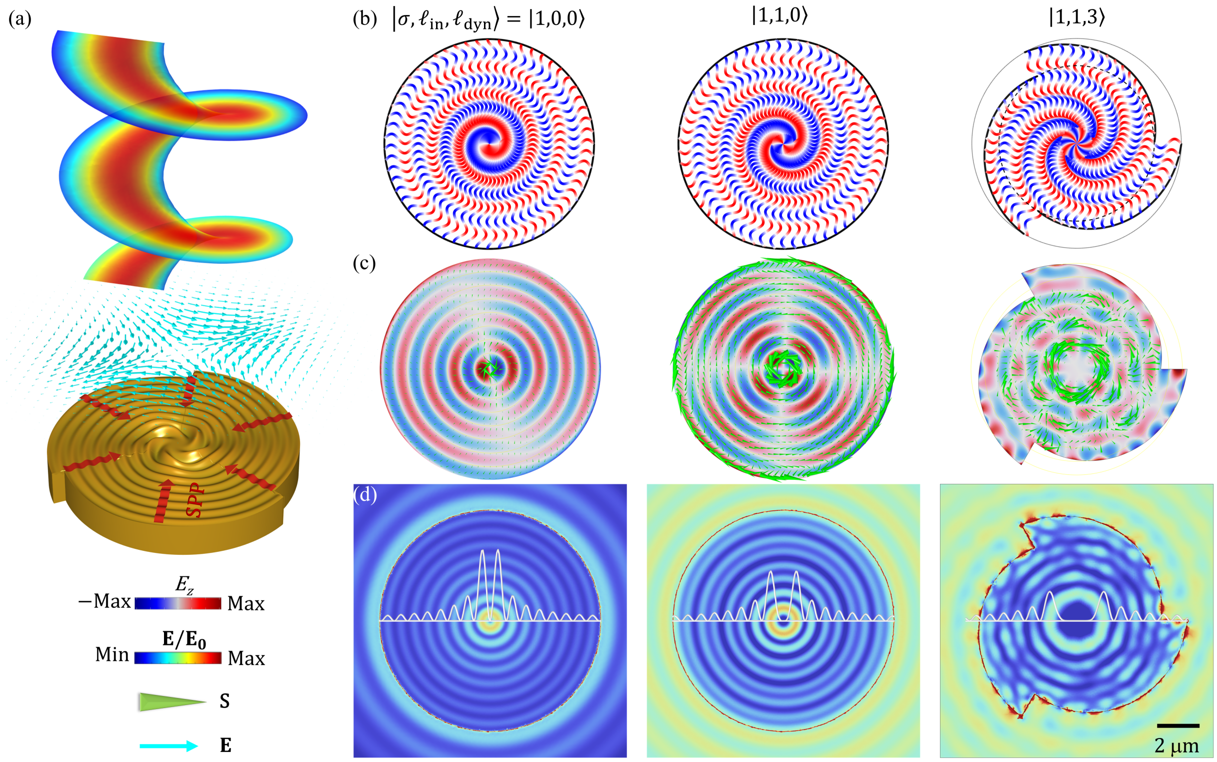

Figure S1: **Geometric- and dynamic-phase-driven topological charge manipulation in a plasmonic vortex lens. (a)** Configuration of the tri-spiral nanolens under vortex-beam illumination. SPPs are launched at the rim and propagate radially inward to form a plasmonic vortex (PV). The cyan arrows indicate the electric field. **(b)**, Principle of phase addition for PV excitation. The illumination provides a geometric phase set by the spin (left) and orbital (right) indices, which fix the initial SPP phase around the rim as $e^{i(\sigma+\ell_{\text{in}})\theta}$. The designed outer/inner radius difference (right, $\Delta r = \ell_{\text{dyn}}\lambda_{\text{SPP}}$) contributes a dynamic phase and leads to an initial phase $e^{i\ell_{\text{dyn}}\theta}$. The two phases add to select the vortex channel (sum rule) $\ell_{\text{tot}} = \ell_{\text{in}} + \sigma + \ell_{\text{dyn}}$. **(c)**, Full-wave simulation of the out-of-plane field E_z at the metal surface, showing the ℓ_{tot}-fold azimuthal phase twist. The green arrows depict the time-averaged Poynting flux **S**, whose azimuthal circulation evidences vortex energy flow. **(d)**, Corresponding amplitude map $|E|/E_0$ compared with a standard Bessel profile $J_{\ell_{\text{tot}}}(k_\rho r)$ (white lines) using $k_\rho(\lambda)$ from the SPP dispersion. Scale bar: $2\,\mu$m.

2. Azimuthal Offset Effects in Plasmonic Vortex Cavities

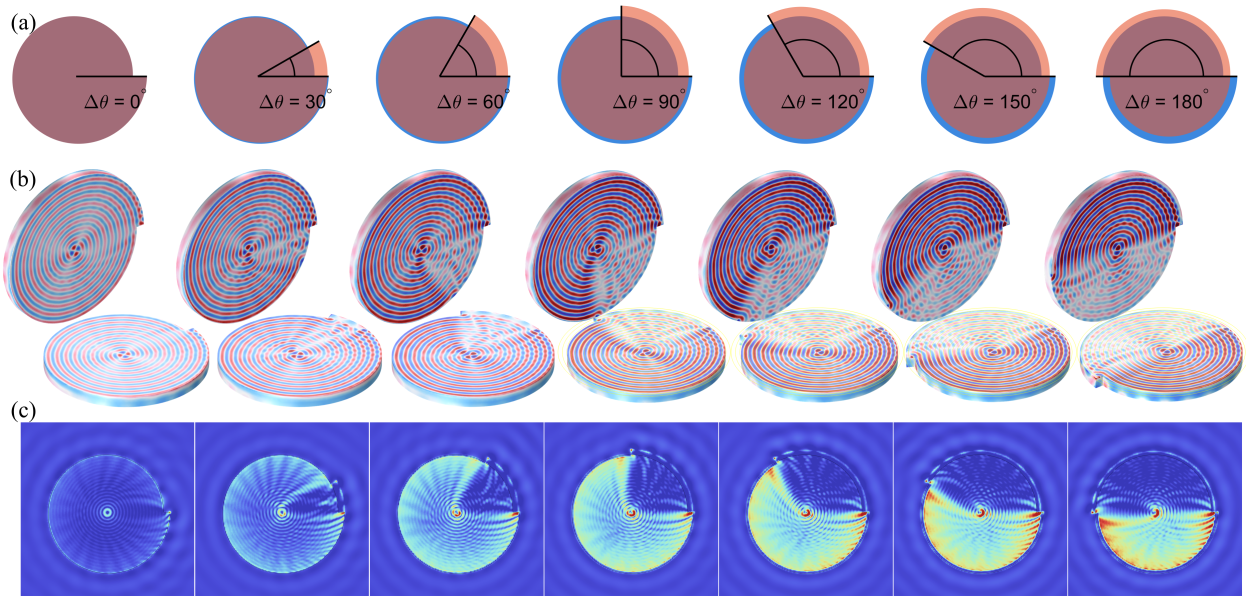

Figure S2: Azimuthal offset effects in plasmonic vortex (PV) cavities: structure, instantaneous phase, and amplitude distributions. **(a)** Schematic of the circular MIM (metal–insulator–metal) cavity structure, with metal disks having spiral edges and an azimuthal offset angle $\Delta\theta$ (from left to right: 0°, 30°, 60°, 90°, 120°, 150°, and 180°). **(b)** Instantaneous vertical electric field E_z for each $\Delta\theta$, showing the overall phase vortex inside the cavity. **(c)** $|E|/E_0$ in the cavity plane.
S

Discussion: Figure S2 illustrates the effects of azimuthal offset ($\Delta\theta$) on the plasmonic vortex (PV) cavities. In part (a), the schematic shows the structure of the MIM cavity, where the metal disks possess spiral edges with varying offset angles. As the offset increases, the interaction between the two metal disks results in a distinctive opening at the outer edge of the cavity, creating a wedge-like region. In part (b), the instantaneous vertical electric field (E_z) is shown for each offset angle, where the phase vortex structure becomes more prominent. Part (c) shows the normalized amplitude distribution $|E|/E_0$ in the cavity plane, revealing the Bessel-like bright rings characteristic of PVs. At the open wedge, there is a noticeable truncation and dimming of the rings.